ASSOCIATION BETWEEN IMU BASED ACCELEROMETRY ON THE TIBIA AND VERTICAL GROUND REACTION FORCE DURING DROP LANDING

Aaron Seth Clapp

A thesis submitted to the faculty at the University of North Carolina at Chapel Hill in partial fulfillment of the requirements for the degree of Master of Arts in the Department of Exercise and Sports Science (Athletic Training) in the College of Arts and Sciences.

Chapel Hill
2020

Approved by:

Courtney Chaaban

Alyssa Evans

Jason Mihalik

Darin Padua

Brian Pietrosimone

ABSTRACT

Aaron Seth Clapp: Association Between IMU Based Accelerometry on the Tibia and Vertical Ground Reaction Force During Drop-Landing
(Under the Direction of Brian Pietrosimone)

Peak vertical ground reaction force is a fundamental biomechanical variable often used to assess lower extremity injury risk. Currently, the tools to measure vGRF are not cost effective. Therefore, the purpose of this study is to determine the association between the variables related to IMU-based accelerometry and vGRF as measured from a research grade force-plate during a drop-landing task. Correlations were run on the averages of the 8 trials for peak vGRF to MVA and MMVAD in the right, left, dominant, and non-dominant limb. The non-dominant limb showed the greatest correlation of peak vGRF to MVA ($r=0.803$, $p<0.01$) and MMVAD ($r=0.779$, $p<0.01$). The dominant limb showed the lowest correlation of peak vGRF to MVA ($r=0.573$, $p<0.01$) and MMVAD ($r=0.563$, $p<0.01$). The strength of the association between accelerometry and vGRF during a drop landing may be limb dependent. The strongest associations between vGRF, MVA and MMVAD were in the non-dominant limb.

TABLE OF CONTENTS

LIST OF TABLES vii

LIST OF FIGURES viii

CHAPTER 1: INTRODUCTION 1

Background 1

Gaps in the Literature 2

Purpose and Aim of the Study 3

Research Question 1 3

Hypothesis 1 3

Research Question 2 3

Hypothesis 2 4

CHAPTER 2: LITERATURE REVIEW 5

Altered Biomechanics Following ACL Injury: The Impetus for this study 5

Importance of the study of biomechanics 5

Problem with ACL Injury 5

Biomechanical abnormalities of ACLR individuals 6

Vertical Ground Reaction Force 6

Knee Flexion Angle 7

Sagittal Knee Moments 8

Drop Landing Biomechanics 9

The Need to Optimize Biomechanics after Injury 10
Efforts to collect Biomechanics in the Real World 10
Inertial Measurement Units 10
Pressure Insoles 12
Nanocomposite Piezoresponsive Foam Sensors 13
Overview 14
Accelerometry 15
Background 15
Analysis of Accelerometer Data 16
Accelerometer use in Prior Gait Biomechanical Research 17
Next Steps 19
Conclusion 20
CHAPTER 3: METHODS 21
Study Design 21
Participants 21
Drop-Landing Analysis 22
Drop-Landing Protocol 22
Vertical GRF Data Extraction and Processing 23
Vertical Acceleration Data Extraction and Processing 24
Statistical Analysis 25
CHAPTER 4: RESULTS 26
Between Limb Differences for Peak vGRF, MVA, MMVAD 26
Correlations between Peak vGRF and MVA, MMVAD 27

CHAPTER 5: DISCUSSION 28
Analysis of the Hypothesis 28
Effects of Limb Dominance on the Measurement 28
Alternative Means of Correlating vGRF and Accelerometer Data 30
Using the Max Resultant versus the Vertical Axis of the Accelerometer 30
Utilizing Multiple Accelerometers versus One Accelerometer 30
Clinical Relevance 31
Limitations 31
Future Direction 32
Conclusion 32
TABLES AND FIGURES 33
BIBLIOGRAPHY 50

LIST OF TABLES

Table 1: Participant Demographics..35

Table 2: Participant Averages of the Variables for the Left and Right Side 36

Table 3: Participant Averages of the Variables for the Non-Dominant and Dominant Side.........37

Table 4: Correlative Measures for MVA in the Left and Right Limb 38

Table 5: Correlative Measures for MVA in the Non-Dominant and Dominant Limb 41

Table 6: Correlative Measures for MMVAD in the Left and Right Limb....................................44

Table 7: Correlative Measures for MMVAD in the Non-Dominant and Dominant Limb...........47

LIST OF FIGURES

Figure 1: Overlay of Vertical Accelerations from the Accelerometer and Vertical Ground Reaction Forces from the In-Ground Force Plates 33

Figure 2: Fourier Transformation of the Accelerometer Data 34

Figure 3: Peak vGRF and MVA Correlation for the Left Limb 39

Figure 4: Peak vGRF and MVA Correlation for the Right Limb 40

Figure 5: Peak vGRF and MVA Correlation for the Non-Dominant Limb 42

Figure 6: Peak vGRF and MVA Correlation for the Dominant Limb 43

Figure 7: Peak vGRF and MMVAD Correlation for the Left Limb 45

Figure 8: Peak vGRF and MMVAD Correlation for the Right Limb 46

Figure 9: Peak vGRF and MMVAD Correlation for the Non-Dominant Limb 48

Figure 10: Peak vGRF and MMVAD Correlation for the Dominant Limb 49

CHAPTER 1: INTRODUCTION

Background

Following lower extremity injury, specifically anterior cruciate ligament (ACL) injury, individuals demonstrate altered drop-landing biomechanics compared to uninjured controls due to impaired neuromuscular control of the lower extremity.[1–4] Aberrant drop-landing biomechanics may increase the risk of sustaining a second ACL injury following ACL reconstruction (ACLR).[4,5] Proper lower extremity energy attenuation is critical for ensuring that joint tissues are not overstressed during dynamic movements.[6,7] Therefore, the ability to easily measure loading of the lower extremity during dynamic movements, such as drop-landing, is critical for determining injury risk in individuals with knee injuries and those at risk for knee injuries.

Vertical ground reaction force is defined as the force exerted on the body in the vertical direction by the ground during stance phase. Greater vGRF during landing may increase the forces exerted to structures of the knee and increase the risk for injury. Lesser knee and hip flexion angles during drop-landing with high vGRF may further increase the risk of injury.[4,7,8] Peak vGRF is an important biomechanical variable associated with knee injury risk, therefore has been a target for drop-landing biofeedback interventions which seek to decrease peak vGRF during drop-landing.[9–13] However, vGRF is most commonly analyzed within a research laboratory setting with expensive equipment including forceplates.[4,14] There is limited research evaluating affordable real-world devices for collecting measures that correlate with vGRF during drop-landing. In a real-world setting, such as in a clinic, it is difficult to find sufficient alternatives for helping correct altered drop-landing patterns following injury.

In recent research, accelerometers have shown the potential to be used to accurately estimate peak vGRF.[15] Due to the high cost of the equipment used to measure vGRF in a laboratory setting, accelerometers could prove to be a cheaper option for estimating vGRF in the real world. Determining the strength of the association between accelerometer variables and vGRF could the lead to the use of this data in the real world to provide real-time feedback. There has been some success with using an accelerometer mounted on the top of the shoe to predict vGRF during various running speeds.[16] While a strong cross-correlational coefficient was reported between the predicted value of vGRF and the observed vGRF (r=0.99), the study used a neural network model to achieve this strong correlation.[16] The potential of finding a strong correlation between peak vGRF and the data from an inertial measurement unit (IMU) based accelerometer could lead to a more clinically feasible method for using accelerometers to estimate important vGRF outcomes during drop-landing or other dynamic activities.

Gaps in the Literature

Currently, there is limited research evaluating the association between individual variables captured by a single accelerometry signal within an IMU to vGRF data from research grade force plates during drop landing. Often, the data from the accelerometers are input into a neural network model in order to try and predict vGRF during varius running and walking tasks.[16] There are also inconsistencies with accelerometer placement leading to different results at the hip (r=0.73),[17] tibia (r=0.75), [15,18] and the top of the shoe (r=0.99, neural net compared to actual vGRF)[16] during those tasks. Due to previous literature we have chosen to place the accelerometer on the tibia to because it shows a higher correlation with vGRF during walking and running tasks.[15,17] The high correlation with the placement on the tibia in those dynamic tasks demonstrates that the best correlation during a drop-landing task may come from the placement on the tibia.

Purpose and Aim of the Study

Therefore, the purpose of this study was to determine the association between the variables related to IMU-based accelerometry placed on the tibia and vGRF as measured from a research grade force-plate during a drop-landing task.

Research Question 1

Does the maximum vertical acceleration (MVA) from the x-axis of the accelerometer signal derived from the IMU located at the middle of the tibia correlate with in-ground force plate peak vGRF collected during a drop-landing task, for the right and left limbs, as well as the dominant and non-dominant limbs?

Hypothesis 1

There will be a strong positive correlation between the MVA and the peak vGRF from the force plate during the drop-landing task the right and left limbs, as well as the dominant and non-dominant limbs.

Research Question 2

Does the minimum to maximum vertical acceleration difference (MMVAD) from the x-axis of the accelerometer signal derived from the IMU located at the middle of the tibia correlate with the peak vGRF, during a drop-landing task, from the in-ground force plate, for the right and left limbs, as well as the dominant and non-dominant limbs?

Hypothesis 2

There will be a strong positive association between the MMVAD and the peak vGRF from the force plate during the drop-landing task in the right and left limbs, as well as the dominant and non-dominant limbs.

CHAPTER 2: LITERATURE REVIEW

Altered Biomechanics Following ACL Injury: The Impetus for this study

Importance of the study of biomechanics

Biomechanical analyses are commonly used to study movement differences between controls and patient populations of interest.[19–21] Gait analysis specifically allows for studying injury prevention[22] and improvements in movement from rehabilitation[23] as well as disease etiology and pathology.[20,24–26] Following anterior cruciate ligament (ACL) reconstruction, the biomechanics during gait are altered which impacts the ability to absorb load at the joint.[19,20] Compensations in gait could increase the risk of ACL re-injury[19,20] or the development of post-traumatic osteoarthritis.[25–28]

Problem with ACL Injury

Anterior cruciate ligament (ACL) injury has been thought to occur due to two philosophies. One is that decreased neuromuscular control along with increased valgus joint loading can lead to ACL injury.[29] Decreased neuromuscular control specifically refers to the muscle groups around the knees inadequate means of dissipating forces and torques.[29] The other thought is that during non-contact ACL injury landing on an extended knee puts an individual at a high risk of ACL rupture, especially if accompanied by increased anterior translation of the tibia, internal tibial rotation, or valgus rotation.[30] A recent epidemiological study has shown that nearly 120,000 ACL injuries occur every year.[31] ACL injury accounts for nearly 50 percent of all the knee injuries that occur at the high school or collegiate level of athletics.[31] It is estimated that ACL reconstruction and rehabilitation costs come close to 1 billion dollars nationwide.[31] Female high school athletes have a higher incidence of 0.081 ACL injury per 1000 exposures compared to male athletes who have 0.05 ACL injuries per 1000 exposures.[32]

ACL injury is common and the lasting effects after injury can lead to further pathologies that will impact long-term health of the patient. Muscle deficits and biomechanical abnormalities that persist following injury and reconstruction can lead to post-traumatic osteoarthritis (PTOA).[19] The abnormalities being discussed are seen during an individual's gait following ACLR. These gait changes following ACL reconstruction (ACLR) have been found as risk factors for early onset PTOA or secondary ACL injury.[19,20] PTOA can show as early as 5 years post reconstruction and close to 40 percent develop PTOA within 10 years.[19,33] The development of interventions to restore pre-injury biomechanics could be an important and effective intervention for improving gait biomechanics and mitigating the risk of PTOA following ACLR.

Biomechanical abnormalities of ACLR individuals

<u>Vertical Ground Reaction Force</u>

Ground reaction force is defined as the amount of force exerted on the body by the ground during stance phase of gait. Ground reaction force is broken into three components, anterior-posterior, mediolateral, and vertical components.[34] Vertical ground reaction force (vGRF) is defined as the vertical component of force applied to the lower extremity during three phases of gait: weight acceptance, mid-stance, and push off.[14]

During gait the peak vGRF during weight acceptance phase (i.e. impact peak) is thought to be indicative of long lasting joint health and subsequently is a common studied gait component.[35] Individuals with ACLR have a gait pattern with less vGRF during the initial peak (weight acceptance) and greater vGRF during the mid-stance of gait.[35,36] It has been shown in research that greater peak vGRF during the weight acceptance phase of gait has shown lesser type II collagen turnover (breakdown relative to synthesis) in the involved limb.[36] When an individual demonstrates a lesser peak vGRF during the first 50% of stance, the individual has greater type II collagen turnover, leading to early onset PTOA.[36] It is important to understand the relationship between the ACLR limb and the uninvolved limb. Rather than the biomechanics of the ACLR limb being elevated to the level of the uninvolved, the reverse happens. The uninvolved limb often demonstrates biomechanics similar to the ACLR limb in terms of showing less vGRF during the first 50 percent of gait.[4,20,26,27,35,36] The changes in the involved and uninvolved leg have been linked to several different areas that relate to the patients overall health and well being following ACLR. It has been shown that improper loading mechanics can lead to lower patient reported outcomes, cartilage deformation, and type II collagen breakdown.[28,36–39]

Knee Flexion Angle

Peak knee flexion angle is defined as the maximum knee flexion angle that an individual demonstrates during the first 50% of stance. A lesser peak knee flexion angle is associated with a “stiffened-knee gait” strategy that prohibits proper distribution of load across the joint surface, potentially damaging the area of contact, that has been shown to be detrimental in ACLR individuals.[20,35] If an ACLR individual displays a smaller knee flexion angle the load cannot be distributed across the entire joint surface.[4,20] Knee flexion excursion is a biomechanical measurement describing the total change in knee flexion range of motion over the first 50 percent of gait.[28] Peak knee flexion angle and knee flexion excursion have been used to describe the gait of ACLR patients compared to control groups and to the uninvolved limb of the patient.

When compared to the uninvolved limb, peak knee flexion angle during stance in the ACLR limb is lesser at various time points post-surgery.[4] Over time, the peak knee flexion angle of the ACLR individuals becomes more symmetrical to that of the uninvolved limb.[4] A reason for this could be that the uninvolved limb is actually developing a lesser knee flexion angle to make the body have a more symmetrical gait. In a study comparing the ACLR limb of 22 female participants to the uninvolved limb it was found that patients demonstrated less peak knee flexion even 60 months post-ACLR.[28] In the same study greater knee flexion excursion following ACLR associated with lesser cartilage deformation after gait.[28] Individuals, following ACLR, display less knee flexion excursion, which could lead to greater cartilage deformation.[28]

Sagittal Knee Moments

During gait, the quadriceps eccentrically contract allowing the knee to go into a deeper knee flexion angle to absorb the forces being placed on it. The internal knee extension moment (KEM) (i.e., external knee flexion moment) is used to analyze gait biomechanics following ACLR.[20] The KEM describes the forces the quadriceps must produce to counter the force making the knee go into flexion.

Peak KEM is decreased in individuals with ACLR when compared to a healthy control group.[20] The decrease in peak KEM is referred to as the quadriceps avoidance strategy.[23,28,40] Following ACL surgery the vastus medialis oblique (VMO) is inhibited causing patients to have less of an eccentric contraction during gait;[35] often leaving patients displaying a stiffer knee during gait because the quadriceps are not allowing the knee to go into a greater knee flexion excursion.[35] Differences between in peak KEM have also been shown when comparing an ACLR group to a healthy control.[20] Associations between KEM and cartilage health have also been discussed in literature. Increases in KEM led to increases in T1 and T2 relaxation times on an MRI, which associated with greater cartilage degeneration.[41]

Drop Landing Biomechanics

In a dynamic movement, such as a drop landing task, lower-extremity biomechanics must adapt in order to absorb greater magnitudes of energy.[3] This is key for patients returning from ACL reconstruction because aberrant landing biomechanics are associated with future injury risk.[9] One of the key biomechanical variables often evaluated for injury risk is the peak knee flexion angle during the drop-landing task. Similarly to what was described within gait biomechanics, the peak knee flexion angle is the point of maximum flexion during the eccentric loading phase of the drop landing task.[2,4] Peak knee flexion angle has been associated with changes in peak vGRF during a drop landing phase.[3,4] Greater peak vGRF during a drop-landing task has been associated with individuals described as having a stiff landing.[5] Individuals described as having a soft landing show lesser peak vGRF and a lesser peak knee flexion angle.[5,9] When individuals display lesser knee flexion angle during landing; they also show a lesser external knee extension moment. External knee extension moment refers to the counteractive forces as the knee goes into flexion eccentrically.[2] If the quadriceps are not adequately prepared to fire to achieve a great knee flexion angle to individual will appear to have a stiffened landing as well.[4] Lesser knee flexion is associated with higher vGRF during drop-landing, which may be associated with higher injury risk to lower extremity tissues.

The Need to Optimize Biomechanics after Injury

The development of interventions to restore pre-injury biomechanics could be an important and effective intervention for improving biomechanics and mitigating the risk of re-injury and PTOA following ACLR. Real-time biofeedback is a method used to alter biomechanics that prompt a change to normal movement patterns.[14] Current methods of conducting research regarding real-time vGRF require force plate treadmills or force plates that have highs costs associated with them.[14] Outside of a laboratory setting it is hard to capture real-time feedback given the equipment needed.[34] Due to cost it is hard for some institutions (i.e. rehabilitation clinics, college athletics, other athletic facilities) to outweigh the cost versus benefits of use. If interventions to change gait biomechanics are going to be accessible to the public they must be more cost effective. Progress has been made in the use of insole based pressure sensors and accelerometers to calculate a measure of vGRF during gait.[17,34,42–45]

Efforts to collect Biomechanics in the Real World

<u>Inertial Measurement Units</u>

Inertial measurement units (IMU) combine three small electrical devices together and are used to orient an object's relative 3-dimensional (3-D) position in space by measuring linear and rotational accelerations.[46] The three devices that compose the IMU are an accelerometer, a gyroscope, and a magnetometer.[47] The gyroscope measures the rotational accelerations of the IMU.[47] A magnetometer is used to measure the strength and location of changes in the magnetic field around the device, acting similarly to a compass. The accelerometer measures inertial acceleration or movement and when combined with the magnetometer and gyroscope can give a 3-D representation of the limb in space.[47] Data collected from each of the three components can be transmitted wirelessly to an external device for real-time analysis or can be stored within the IMU for post-processing purposes.[48] Depending on storage, transfer, capture rate capabilities, and affiliated software, the cost of an IMU varies between $15 and $900.[49,50] Due to the cost effectiveness compared to standard laboratory gait analysis equipment, IMUs may have the potential to be purchased by clinicians to study joint position and the biomechanics of gait in real time.[47]

IMUs have been used to estimate variables of human biomechanics (i.e., phase of gait, stride length, swing phase duration, and gait asymmetries),[48] both within and outside of a laboratory setting.[43,47] Distinguishing between phases of stance (i.e., heel-strike, midstance, and toe-off) is important to understand when loading is occurring.[16,47] Although determining phases of stance is easily done by analyzing ground reaction forces, this limits the analysis to a laboratory setting. Recently, using time overlap of the vGRF data and the peak acceleration data, the anterior-posterior axis of the accelerometer in the IMU was used to estimate phase of stance.[16] Using this same anterior posterior axis of the accelerometer, but adding other known variables such as gait speed, stride length and swing and stance phase time-durations were also estimated. [48] Comparing this information acquired from the IMUs between limbs of an individual subject allowed for determination of limb asymmetry.[48]

Due to the complexity of the algorithms that must be conducted to integrate the data from the three components of the IMU, it is difficult to use and understand from a clinical setting.

Pressure Insoles

Pressure insoles[42,51] may be an alternative and effective way of analyzing gait. Within an insole, pressure sensors are used to turn the mechanical pressure into an electrical signal.[42] Pressure is defined as the amount of force divided by the area under it. Easily understood, the greater the force put into a specific area the greater the pressure, but as surface area increases, pressure decreases. Insoles vary in the amount of pressure sensors per brand of insole with some consisting of 1 sensor with others having up to 99 sensors.[42] Depending on the number and position of pressure sensors within the insole, the company, and data storage and transmission unit, the prices of the insoles can cost a couple thousand dollars. Pressure data from the insoles are different between insoles, but data can either be collected and then downloaded to a computer while other have the capability to connect to a phone application via WiFi or Bluetooth.[42,51] Compared to IMUs, pressure insoles are more easily analyzed due to the fact that a mechanical load is turned into an electrical signal.[34] The signal from pressure insoles allows for easy to understand signal that maps out similarly to that of vGRF due to the input of one variable versus multiple variables from the IMU.

Pressure insoles have been used to analyze gait kinetics (vGRF, loading rate, impulse, contact time and pressure distribution).[51] Pressure insoles can be placed into a shoe and measure the plantar distribution across the insole and collect a voltage signal that has been correlated with vGRF, ground contact time, and time to initial peak.[42,51,52]

Loadsol, which is made up of one sensor spanning the width of the insole, showed a high interclass coefficient (ICC) 0.61-0.97 for impact peak of vGRF during running when compared to force plate data for impact peak.[51] Loadsol pressure insole only showed an ICC value lower than 0.90 when the collecting frequency was 100 Hz, when this was increased to 200 Hz the ICC values were all greater than 0.90.[51] Similarly, high associations (r = 0.80) were found between the voltage signal and force plate sensors in OpenGo sensors, although ICC values were not calculated.[42] F-Scan Insoles showed high reliability when compared to impact peak at the toe, midfoot, and forefoot sensor placement with a ICC above 0.83. The heel sensor only showed a ICC of 0.68, suggesting only moderate reliability of this sensor for associating with impact peak of vGRF.[52] The finding is specifically important because forces produced at the heel during initial contact are often described as the initial peak of vGRF during the first 50 percent of gait.[52]

Despite promising applications of these insoles, there are limitations for clinical or other real-world use. With this high cost coming per set of pressure insoles it is difficult for rehabilitation clinics to buy multiple insoles and the software needed to analyze these data.

Nanocomposite Piezoresponsive Foam Sensors

Nanocomposite quasi-piezoelectric foam (NQPF) sensors are a different type of sensors that predict kinetics. Initially, the NQPF sensors were placed inside football helmets to detect impact forces during game play in order to detect when a certain force threshold had been reached so the clinician could check for concussive symptoms.[34] As the head hits the NQPF sensors an output voltage proportional to the load is generated and recorded to a microchip hard-wired to the foam sensors themselves.[34] The voltage output is then used as an input of a predictive model created to estimate variables of load.[34] By placing 4 of sensors into an insole that is then placed into, a shoe, these same sensors are now being used to estimate ground reaction forces during human movement.[34]

Voltage signals from each sensor within the insole were collected during walking and running and used to predict anterior-posterior, medio-lateral, and vertical GRF throughout the entire gait waveform.[34] vGRF provided the lowest mean average error percentage (2.31%) between the predicted measurements of force using the piezoelectric sensors and the measured force from the instrumented treadmill.[34] Although accuracy measures were collected along one set walking speed, it is hard to tell whether various walking speeds would affect this mean average error across subjects.[34] Other methods of data collection such as IMU's and pressure insoles were tested across multiple walking speeds and that is why walking speed is only a limitation for the NQPF sensors at this time.

While the foam insoles are still in the beginning stages of development, the low cost of the foam insoles make them a promising avenue for future real-time and real-world gait analysis.

<u>Overview</u>

Although these various forms of vGRF measuring devices show promise for the future in terms of real-world applications, limitations impacting usability exist for each of these devices. Limitations in the price of these measurement tools and the software that they require should require other methods to be further explored.

Accelerometry

Background

Accelerometers have the potential to provide a low cost and accurate way of analyzing movement. There are two forms of accelerometers, uniaxial and triaxial accelerometers.[15] Uniaxial accelerometers are capable of measuring data along a single axis; the axis is dictated by the positioning of the accelerometer on the moving object.[18] Triaxial accelerometers record data across the axial, mediolateral, and anterior-posterior axes.[18] The additional data measured from the triaxial accelerometers, compared to the uniaxial accelerometers, are necessary to provide a better chance to estimate characteristics of the relative complex nature of human movement.[18] Each of the three axes are susceptible to noise, or data unattributed to gait that is being analyzed. Careful placement of the accelerometer on the subject of interest can help to reduce unwanted noise, however, often the resultant of the axes is filtered with a low pass filter prior to analysis.[53]

Compared to IMUs, pressure insoles, and NQPF sensors, accelerometers can be dramatically lower in cost; depending on storage and transmission capabilities a standard triaxial accelerometer can be purchased for less than $10 to as much as $60.[54] In fact, the low cost and high potential of accelerometers has already led to the commercialization of "instrumented shoes" that have accelerometers embedded into the sole of otherwise standard running shoes. If accurate predictive models using accelerometry data could be created to be valid and reliable, analyzing human kinetics and kinematics would be feasible in a clinical setting.

Analysis of Accelerometer Data

Accelerometers have the potential to estimate both foundational and complex kinetics and kinematics. Depending on the variable of interest, accelerometers can be used independently or in tandem with other accelerometers.[15,17] Common ways of processing data are: (1) Comparing discrete points from one accelerometer axis to a biomechanical variable of interest,[17] (2) comparing relative accelerations between multiple accelerometers placed on unique segments,[15,44] or (3) creating a model using a neural network to predict the variable of interest.[16]

When dealing with a "simple" direct variable such as vGRF, a single accelerometer can be used to associate and find a predicted value. However, more complicated kinetic and kinematic measurements (i.e., joint angles) can be approximated by using data from multiple accelerometers placed on unique segments simultaneously.[43] The most robust way to approximate a variable of interest using accelerometer data is by creating a predictive model.[16] Predictive models allow for an unlimited number of data inputs. Meaning, that all axes of multiple accelerometers can be used to inform an approximation of the variable of interest. Whether it is in literature around pressure insoles, IMUs, or accelerometer data a neural network (NN) model is often used to predict variables along the vGRF graph from the data collected by these various collecting tools.[16,34] NN models are uniquely designed for the data set that is being collected, taking into account the input variables of interest to produce an output variable (i.e. vGRF).[16]

Accelerometer use in Prior Gait Biomechanical Research

Accelerometry data has successfully been correlated with multiple biomechanical variables of interest, especially with cyclical tasks such as walking and running.[16–18,55] During the cyclical task of walking, the acceleration of the tibia is a repeated pattern that coincides with each step through a variety of peaks and valleys of the accelerometer data.[53] When an individual is not taking a step there is still a noise present within the signal.[18] Accelerations collected at higher frequencies must use a low pass filter with post processing to cancel out the noise, or excess signal when the accelerometer is not moving.[18] Only after the use of a low pass filter can the true accelerations be appreciated.

Two of the most relevant variables for this paper are peak positive tibial axial acceleration and trunk acceleration and the relationship between these variables and vGRF.[53] All three of these variables are measured directly from the accelerometer and are used to correlate with other kinetic and kinematic variables.[53] Peak positive tibial acceleration (TA) is measured by summation of linear acceleration of the tibia caused by ground reaction forces, acceleration of gravity, and angular motion.[18] Peak TA has shown correlation during running between the stride length, cadence, and running velocity but the correlation to vGRF was not as significant.[18] It was predicted that the axial component of the accelerometer data would change in relation to foot strike but that was not the case.[18]

Trunk acceleration is another critical variable that can be collected with the use of accelerometers to correlate with various gait characteristics.[17,56] The major gait characteristics that trunk acceleration has been associated with are vGRF, cadence, and stride length.[17,56] When measuring trunk acceleration the triaxial accelerometer was attached to a belt, secured around the waist for collection.[56] Trunk acceleration was capable of collecting cadence and stride regularity by looking at the unbiased and biased accelerometry data, although no accuracy measure was reported.[56] Stride length and regularity were measured by taking the amount of time from initial footfall to the ipsilateral footfall.[56] Trunk acceleration has also been used to correlate with vertical forces attenuate up the lower extremity.[17] The peak loading rate and the peak vGRF were both collected and correlated with trunk acceleration, r=.85 and r=.76 respectively.[17] The correlations values demonstrate that accelerometry at the hip have positive correlations with that of the vGRF data from force plates.

Accelerometry has been found to correlate with loading rates and peak vGRF. Loading rate describes the rate that force is exerted onto the limb, therefore should be associated with an expression of acceleration in the axial component of acceleration.[18] Strong positive correlations with loading rates are much easier variables to find association with because loading rates are a form type of acceleration.[18] Accelerometers placed at both malleoli have been correlated with the acceleration of the ankle during running tasks.[44]

Finding a direct correlation to vGRF from accelerometry is more difficult to do, and subsequently attempted less frequently as vGRF is not a direct measurement of acceleration. However, due to the correlation between accelerometers and variables of gait, such as tibial acceleration and loading rate, it is believed that there will be a correlation between raw accelerometry data and vGRF. Additionally, by using a neural network model to create a predictive model of vGRF estimations of vGRF can be good. The signals from accelerometers have had some success with using the raw data to correlate to vGRF.[17,44,53] Correlations to vGRF from accelerometry data have been found at various body segment attachments but some of the best results have been shown from placement along the tibia, malleoli of the ankle, and shoe.[16,18,44] Although the most successful way was using peak acceleration within a NN model, good results were found with the predictive model having a correlation of $r = 0.99$ at various running speeds to the vGRF data.[16] If vGRF can be assessed using accelerometry this could open the door to studying other limb kinetics such as knee flexion angle or KEM. Vertical GRF has been correlated with knee flexion angle and KEM.[4,20,27] An individual displaying lesser knee flexion angle will also have a lesser KEM due to the quadriceps avoidance strategy.[20,35] Peak KFA and KEM can both directly be correlated back to the vGRF that they are experiencing during gait. By altering the vGRF an individual would then be able to change their gait to display a greater peak KFA and KEM. Accelerometry could prove to be a cost effective tool for measuring vGRF and thus could be useful in a clinical setting for altering gait biomechanics.

Next Steps

Raw accelerometry data could prove to have correlative factors to that of vGRF or loading rates of the lower extremity.[15,17,44] The first step involves finding the specific points of the raw accelerometry data that correlates with vGRF.[15] While data from a triaxial accelerometer placed on the ankle has shown promise in this regard,[15] shoe based accelerometry has yet to be explored as an alternative measurement tool for gait biomechanics research.

Conclusion

The current state of biomechanics analysis requires laboratories with advanced equipment that is out range in cost for most rehabilitation centers. Physical therapist or athletic trainers in clinics are unable to properly change a patient's gait biomechanics purely because of cost of the equipment necessary. There is a necessity for real-world applications of this technology so compensations during gait can be fixed in a clinic setting. Accelerometry may be a cost effective tool that can be used as an alternative measurement tool for changing these gait patterns following injury. The first step to achieving this goal is to discover what portions of the data best correlate with the vGRF.

CHAPTER 3: METHODS

Study Design

This study was a descriptive cross-sectional study consisting of a single testing session, during which all outcomes (i.e., peak vGRF, maximum vertical acceleration (MVA), and the minimum to maximum vertical acceleration difference (MMVAD)) were collected during a drop-landing protocol. Peak vGRF from each drop-landing, measured using an in-ground force plate (FP406010, Bertec Corp) was selected as the criterion variable, while variables of MVA and the MMVAD from an accelerometer within an IMU were chosen to be predictive variables. All participants had one IMU placed on each tibia (Blue Trident, IMeasureU, Auckland, NZ) for the entirety of the session. The IMUs were placed on the flat aspect of the proximal anterior medial portion of the tibia. The top of the IMU was placed 5 cm distal to the tibiofemoral joint line as palpated. All participants provided written informed consent approved by the Institutional Review Board at the University of North Carolina at Chapel Hill prior to participating in any research related procedures.

Participants

We enrolled a convenience sample of 27 individuals from the university community between the ages of 18-35 years of age. All participants were required to be currently engaging in unrestricted physical activity, which included at least 30 minutes of physical activity three times per week. We excluded individuals with: 1) any lower extremity injury/surgery within the past 6 months; 2) known pregnancy (due to alterations in biomechanics; and 3) an inability to participate in physical activity. We estimated the ability to detect a statistically significant association between accelerometer data and vGRF if a moderate effect ($r=0.52$) was present in 27 individuals (two-tailed test with 80% power and $\alpha \leq 0.05$).

Drop-Landing Analysis

Drop-Landing Protocol

Participants then completed a drop landing protocol on to two 40x60 cm force plates (Bertec, Columbus, OH, Model FP406010). Participants were allowed practice drops to allow for them to become familiar with the process. Participants were instructed to jump forward off a 30 cm box, placed approximately 50% of the participant's height away from the force plates. Participants were instructed to land with one foot in each force plate. Approximately 3 practice drops were allowed to each participant, unless the researcher felt that the participant needed more practice. The in-ground force plates were calibrated and zeroed 30 minutes prior to data collection and were zeroed again immediately prior to the 8 drop-landing trials. Vertical GRF and vertical accelerations from the accelerometer were collected simultaneously during the 8 drop-landing trials. If an error occurred during one of the drops (e.g., both feet did not land in individual force plate) then the participant was asked to repeat the drop. Vertical GRF data from the force plates were collected and stored using Vicon compatible computer software (Vicon, Nexus, Oxford, UK) for post-session processing. Vertical accelerations were synchronized to the computer software (Vicon, Nexus, Oxford, UK) as well, although at a lower frequency 50 Hz. The IMU, onboard, collected at a frequency of 1125Hz, so the data from the IMU was then connected to Nexus from post-session processing.

Vertical GRF Data Extraction and Processing

Forces from the in ground force-plates were collected at a sampling frequency of 1000 Hz. Before processing the data, forces collected from Vicon were converted to a C3D file for filtering. The C3D file was then put into Visual 3D Software (C-Motion, Germantown, MD) to run the filtering and analyzing pipelines. This software allowed for the raw force data to be filtered using a low pass 6th order Butterworth filter cut off frequency of 20 Hz. The vGRF cutoff frequency was based upon the fourier transformation which was conducted on the accelerometers. The cut off frequency of 20 Hz was used for both the vGRF and accelerometer data. Filtering of the data was completed in Visual 3D computer software after the cut off frequency was determined. After filtering the forces, Matlab computer software, (Matlab, version R2020a, Mathworks Inc., Natick, Massachusetts, United States) defined each drop as the first 100ms after initial ground contact (>20 vGRF), after manually selecting a point prior to any rise in the vGRF data (as shown in Figure 1). Then the next line of the code in Matlab was added to find the maximum value between initial ground contact and the last point in the 100ms. This value was defined as peak vGRF during the drop-landing task, as indicated by the green arrow in Figure 1. The peak vGRF variable was found for each of the drop-landing trials. For each subject, the average peak vGRF across the 8 drop-landings was then normalized to the participant's body weight and were used as the peak vGRF variable. The averages for peak vGRF for each subject can be seen in Table 2 for the left and right limb and Table 3 for the Dominant and Non-Dominant Limb. Peak vGRF were normalized to each subject's body weight (BW).

Vertical Acceleration Data Extraction and Processing

During the drop landing protocol, the accelerometers from the IMU collected data at 50 Hz, in real time, while synchronized to Vicon software (Vicon, Nexus, Oxford, UK). Onboard the IMU data was collected and stored at a frequency of 1125Hz for post session processing. The data collected within the IMU was then connected to Vicon to receive all of the data, stored onboard, and run an interpolation function so the data was presented at 1250 Hz. Filtering of this data was done through Visual 3D computer software with a cut off frequency of 20Hz with a 6th order low-pass Butterworth filter. A Fourier transformation was conducted on the data in order to determine the previously stated cut off frequency, as seen in Figure 2. Matlab computer software (Matlab, version R2020a, Math-works Inc., Natick, Massachusetts, United States) was then used to analyze the IMU data. Vertical GRF data and vertical accelerations were analyzed using the same Matlab program. The area of interest for the acceleration data was defined as the same 100 ms timeframe once the participant made ground contact (>20vGRF). The code then found the minimum acceleration value and the maximum acceleration value during that timeframe. The maximum acceleration value was identified as the first variable of interest, MVA. The difference between the minimum acceleration value and the maximum acceleration value was identified as the second variable of interest, MMVAD. Both of the variables are represented within Figure 1. Averages of MVA and MMVAD were used for the 8 drop-landing trials for each participant. Subtracting by 9.81 m/s normalized the averages of MVA and MMVAD for the eight trials. The averages of the normalized MVA and MMVAD for each subject can be seen in Table 2 for the left and right limbs and Table 3 for the Dominant and Non-Dominant Limb.

Statistical Analysis

Normality of each variable was assessed via the Shapiro-Wilk test. Dependent t-tests were used to compare the average vGRF for the right vs left as well as dominant vs nondominant limbs. Separate correlations were completed between the average peak vGRF and the averages of both MVA and the MMVAD. A Pearson product-moment correlation (r) was used to evaluate the associations between peak vGRF and both the MVA and the MMVAD. If a variable was non-normally distributed, a Spearman rank order correlation was used in place of a Pearson product-moment correlation. The associations were defined as negligible (0.0-0.29), low (0.30-0.49), moderate (0.50-0.69), high (0.70-0.89), and very high (0.90-1.0).[58] Alpha levels were set to 0.05 for all analyses, which were performed using the Statistical Package for the Social Sciences (SPSS, Version 21, IBM Corp., Somers, NY).

CHAPTER 4: RESULTS

Between Limb Differences for Peak vGRF, MVA, MMVAD

All 27 participants completed the drop landing protocol (Table 1). The average peak normalized vGRF was lesser on the left limb (1.953 ± 0.485 BW) compared to the right limb (2.211 ± 0.487 BW); $t(26) = 4.178$; $P<0.001$; effect size= -0.530. Seven of the participants noted their dominant limb as being the left side. The average peak normalized vGRF was lesser on the non-dominant limb (1.988 ± 0.511 BW) compared to the dominant limb (2.176 ± 0.476 BW), $t(26)= 2.660$; $P= 0.013$; effect size= -0.396. No outliers were found in the data sample for the average peak vGRF. The average MVA was lesser on the left limb (245.125 ± 146.653 m/s/s) compared to the right limb (265.422 ± 141.424 m/s/s), $t(26) = 0.992$; $P=0.330$; effect size= -0.144. The average MVA was lesser on the non-dominant limb (231.598 ± 123.809 m/s/s) compared to the dominant limb (278.949 ± 158.837 m/s/s), $t(26)=2.537$; $P=0.018$; effect size= -0.298. No outliers were found in the data sample for the average MVA. The average MMVAD was lesser for the left limb (298.265 ± 185.560 m/s/s) compared to the right limb (332.548 ± 177.474 m/s/s), $t(26)=1.287$; $P=0.209$; effect size= -0.193. The average MMVAD was lesser on the non-dominant limb (283.347 ± 161.595 m/s/s) compared to the dominant limb (347.466 ± 195.684 m/s/s), $t(26)=2.625$; $P=0.014$; effect size= -0.328. No outliers were found in the data sample for the average MMVAD.

Correlations between Peak vGRF and MVA, MMVAD

Greater MVA associated with greater peak normalized vGRF for the left ($r=0.780$, $P< 0.01$) and right limb ($r= 0.590$, $P<0.01$; Table 4). The correlations can be seen in Figure 3 for the left limb and Figure 4 for the right limb. Greater MVA associated with greater peak normalized vGRF for the non-dominant ($r=0.803$, $p<0.01$) and dominant limb (0.573, $p<0.01$; Table 5). The correlations can be seen in Figure 5 for the non-dominant limb and Figure 6 for the dominant limb.

Greater MMVAD associated with greater peak normalized vGRF for the left ($r=0.764$, $p<0.01$) and right limb ($r=0.576$, $p<0.01$; Table 6). The correlations can be seen in Figure 7 for the left limb and Figure 8 for the right limb. Greater MMVAD associated with greater peak normalized vGRF for the non-dominant ($r=0.779$, $p<0.01$) and dominant limb ($r=0.563$, $p<0.01$; Table 7). The correlations can be seen in Figure 9 for the non-dominant limb and Figure 10 for the dominant limb.

CHAPTER 5: DISCUSSION

Analysis of the Hypothesis

The purpose of this study was to determine if the x-axis of the accelerometer within an IMU sensor could serve as a comparative measure to vGRF from force plates during a drop-landing task. We chose the x-axis due to the alignment and orientation of the IMU when it was placed on the tibia. The x-axis represented the vertical axis of the tibia when the participant was standing. In agreement with our hypotheses, greater MVA and MMVAD were associated with greater peak vGRF. While there was a significant positive association between accelerations as measured by the IMU and peak vGRF, the strengths of the correlations varied between limbs. Overall, the left and non-dominant limbs demonstrated stronger associations compared to the right and dominant limbs, respectively. The differences in the strengths of the correlations for the left and right limb, as well as, the non-dominant and dominant limb are important to consider due to the implications that the x-axis of the accelerometers may not be a reliable measure for vGRF in the dominant limb. Future research will be needed to confirm this hypothesis.

Effects of Limb Dominance on the Measurement

When a participant completes a drop landing task, the body position may change prior to making initial contact with the ground in order to more appropriately absorb the energy imposed on the body.[7] As the participant leaves the box and prepares for landing, the knee starts in slightly flexed position and begins to go into greater knee flexion after they make initial contact.[2,3] During a drop landing task, as the participants may utilize strategies to increase knee and hip flexion angle to lessen peak vGRF.[2,4] Individuals may be more likely to alter their landing strategy on their dominant limb during this novel drop landing task. Furthermore, this task may have been novel to many participants and they may have tested various kinematic strategies to land from the jump more comfortably. A possible explanation of the differences in associations between limbs could come from the representation of the vertical axis of acceleration during a drop-landing task. As the participant begins to go into greater knee flexion to absorb the ground reaction forces, the tibia moves out of a vertical position.[3,7] The change in orientation of tibia, during the 100ms after initial contact where vertical accelerations were measured, may have changed the outcomes of MVA and MMVAD due to the movement. Individuals may have been more likely to make these changes on the dominant limb rather than the non-dominant limb. It is possible that neuromuscular changes were easier to pursue on the dominant extremity.

Our study was focused on participants with no lower extremity injury or surgery within the past 6 months. We believe that the participants within this study demonstrated a drop-landing pattern where they favored their dominant limb during the drop-landing task leading to greater mean values for the three variables of interest. When comparing the means of the separate groups of non-dominant and dominant limb, we determined that there was a difference in the in the peak vGRF, MVA and MMVAD. We saw greater peak vGRF, MVA and MMVAD in the dominant limb. The greater association was found for peak vGRF to the two predictive variables (MVA and MMVAD) in the non-dominant limb than in the dominant. In the study, 7 of the 27 participants were left limb dominant, which would explain the results of seeing a higher correlation of the variables for left versus the right limb.

Alternative Means of Correlating vGRF and Accelerometer Data

Using the Max Resultant versus the Vertical Axis of the Accelerometer

During the study we saw a difference in the strength of the correlations between peak vGRF and the two variables of interest (MVA and MMVAD) for the dominant and non-dominant limbs. The difference could be in part to only correlating the measures of vertical acceleration from a single axis versus using a resultant. As the knee goes into flexion and the vertical orientation of the tibia changes, the true measure of vertical acceleration may be a resultant of the three axes. The resultant is a measure of multiple axes within the accelerometer that can give a more accurate measure of true total acceleration of the limb. With the IMU being placed on the tibia, the x-axis only shows the acceleration forces relative to the vertical orientation of the tibia. Small changes in lower extremity kinematics may impact the ability to correlate these data with the vertical force vector during landing.

Utilizing Multiple Accelerometers versus One Accelerometer

Another alternative method of understanding the true vertical acceleration of the limb could be to use multiple accelerometers placed on different locations of the lower extremity. Multiple accelerometers have been used to try and correlate with vGRF and other biomechanical variables during various tasks such as walking[15] and running.[16,17] The strategy of using multiple accelerometers could help the researcher understand the accelerations and forces throughout the entire limb, instead of one segment during a drop-landing task.

Clinical Relevance

Accelerometers have shown promise in various activities as being an intervention for measuring vGRF with a lower cost than force plates. Our study has shown that in the non-dominant limb there is a high correlation between the vGRF from force plates and the MVA, as well as the MMVAD. Clinically, after the conclusion of this study the correlative measure between the peak vGRF and the two predictive variables MVA and MMVAD show that vertical accelerations from a single placement and axis may be more accurate for the non-dominant limb with a lower peak vGRF, but not for the dominant limb when greater vGRFs are created. More research is needed to determine the validity and reliability of using accelerometers during a drop landing task, so that clinicians can use this lower cost intervention to assess landing biomechanics in patients for return to activity following lower extremity injury.

Limitations

While the results of this study provide insight regarding the use of accelerometers to estimate measure vGRF during a drop-landing task, there were limitations, which should be reviewed. Within our study we only used healthy individuals with no history of lower extremity injury/surgery within the last 6 months. Correlations may be different when reviewing patient populations in terms of an injured and uninjured limb. Other limitations are that the IMU was placed on the participants versus having a fixed placement and orientation and the selection of using the single axis of the accelerometer within the IMU. While there were specific directions into the placement and orientation of the IMU, because the IMU was placed on the individual every session by the research team it is possible that the x-axis could be slightly off from participant to participant.

Researchers should look at the inter-rater and intra-rater reliability of placing the IMU; as well as try to use an IMU with a fixed placement and orientation. With all of these trials taking place in a laboratory setting versus in the real world setting also should be looked at as a limitation to be addressed in future research.

Future Direction

Further research is needed to understand the relationship between using vertical accelerations from an accelerometer and vGRF from force plates. While this study has shown high correlations for some variables of interest, we have also seen that it is not as reliable in the dominant limb. Alternative methods in the future should be explored to better see if they provide a better representation of the association between these variables. The alternative methods include using a max resultant, multiple accelerometers, or having a way to have the accelerometer in a fixed placement and orientation. Finally, in order for this to be used in the future clinical setting, more research should be conducted to evaluate the relationships between peak vGRF and vertical acceleration in an injured populations.

Conclusion

It seems that the strength of the association between accelerometry and vGRF during a drop-jump may be limb dependent. The strongest associations between vGRF, MVA and MMVAD were found in the non-dominant limb.

TABLES AND FIGURES

Figure 1. Overlay of Vertical Accelerations from the Accelerometer and Vertical Ground Reaction Forces from the In-ground Force plates. Figure 1 shows the overlay of the vertical accelerations from the accelerometer (orange line) and the vGRF from the in ground force plates (blue line) after the data was processed during one drop landing. The variables of vGRF, maximum vertical accelerations, and minimum to maximum vertical acceleration difference were determined after selecting the area before the first increase in vGRF. After the vGRF went over 20N the variables were determined within the following 100ms. The green arrow describes the peak vGRF, the red arrow describes the MVA, and the difference between the blue arrows is the variable of MMVAD.

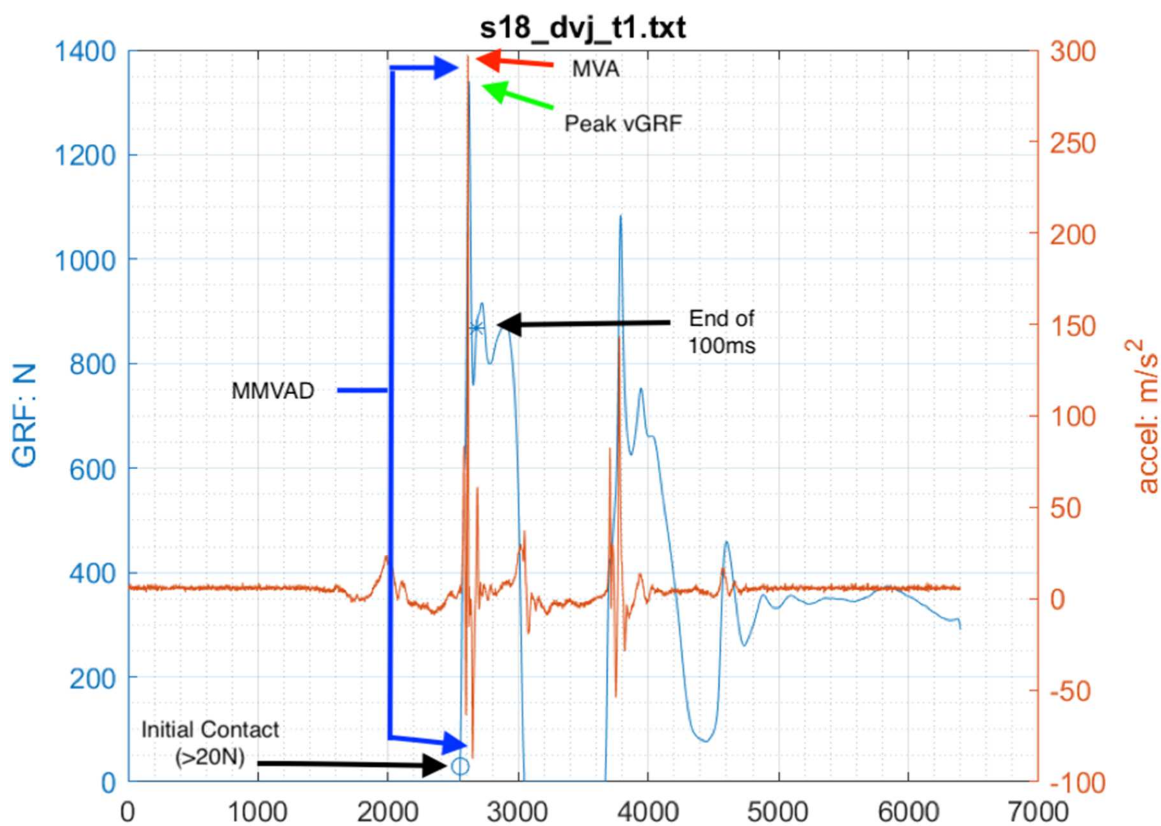

Figure 2. Fourier Transformation of the Accelerometer Data. Figure 3 displays the Fourier transformation of the accelerometer data after it was extracted from the accelerometer. This allowed for a cut-off frequency of 20 Hz in order for a low pass filter to be applied. It was determined that any data collected at a frequency greater than 20 Hz would be excluded as noise.

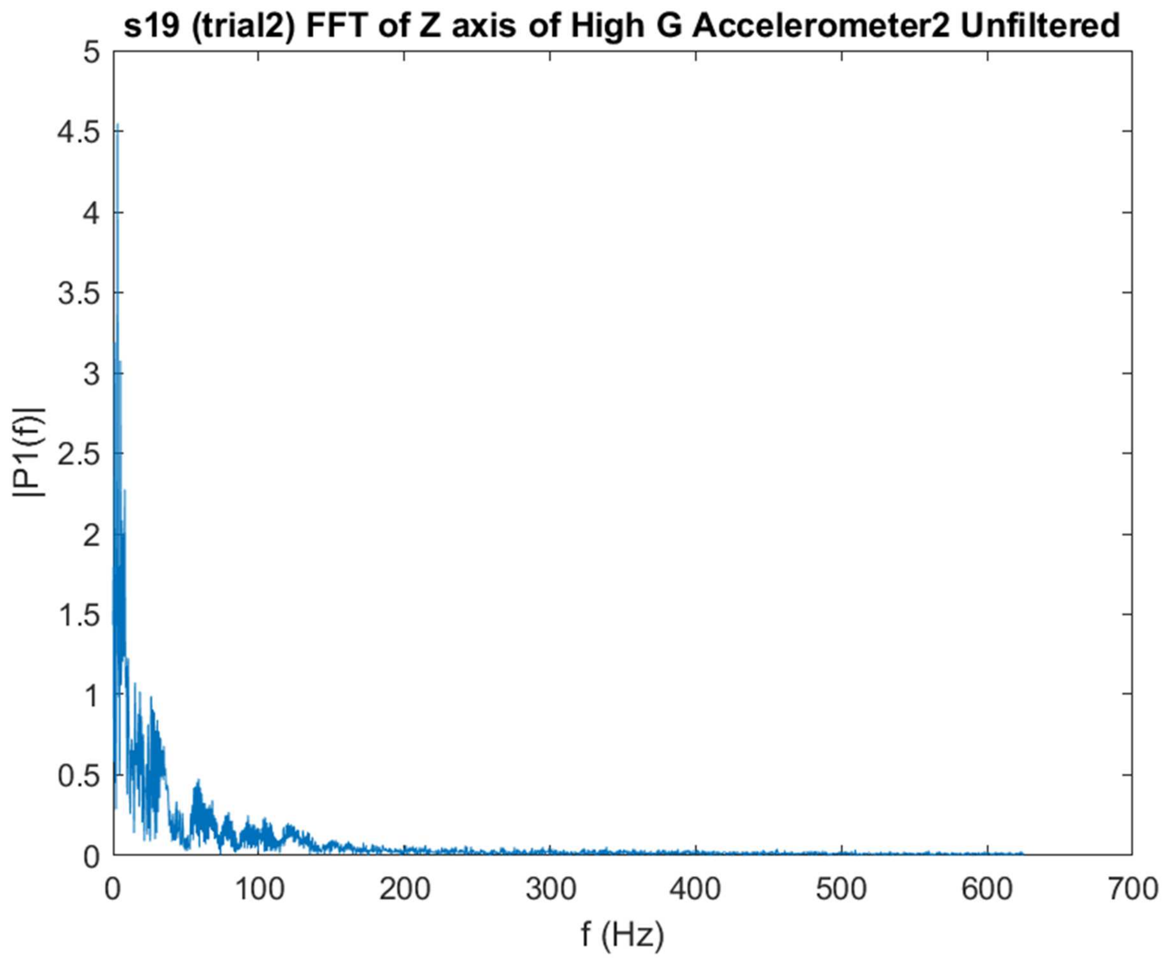

Table 1. Participant Demographics. Table 1 lists out the demographics of the participants enrolled in this study. Table 1 shows the participant's age, sex, height (cm), weight (kg) and the dominant limb. In the table sex is denoted as a 0 or 1 where 1 represents female and 0 represents male. The dominant limb is also denoted as a 0 or 1 where 0 represents the left leg and a 1 represents the right leg.

Participant's Demographics						
Prefix Letter	Number	Age	Sex	Height (cm)	Weight (kg)	Dominant limb
s	18	22	1	170.50	69.40	1
s	19	21	1	165.00	66.40	0
s	20		1	166.00	58.17	1
s	21	20	1	174.00	87.40	1
s	22	20	1	174.20	67.60	0
s	23	21	0	184.50	88.20	1
s	24	23	1	162.50	56.20	1
s	25	20	1	159.50	70.60	1
s	27	19	1	166.60	63.20	1
s	28	21	0	183.50	78.60	1
s	29	18	1	163.50	55.00	0
s	30	20	1	168.00	80.60	1
s	31	22	1	178.00	65.60	1
s	32	21	1	168.50	56.00	0
s	33	20	1	163.00	57.00	1
s	34	21	1	169.20	65.80	0
v	9	20	1	183.00	74.40	0
v	10	21	1	171.00	59.90	0
v	11	18	1	167.64	66.20	1
v	12	20	1	182.88	75.30	0
v	13	19	1	180.34	94.30	1
v	14	18	1	186.00	77.10	1
v	16	20	1	177.80	64.90	1
v	17	18	1	176.00	72.10	1
v	18	20	1	168.00	68.90	1
v	19	19	1	160.03	60.30	1
v	20	20	1	170.00	67.60	1

Table 2. Participant Averages of the Variables for Left and Right Side. Table 2 shows averages of 8 drop landings across each subject for peak vGRF normalized to body weight, Maximum Vertical Acceleration (MVA), and Minimum to Maximum Vertical Acceleration Difference (MMVAD).

Averages of Variables for the Left and Right Limb						
Participant	vGRF (L)	MVA (L)	MMVAD (L)	vGRF (R)	MVA (R)	MMVAD (R)
s18	2.069	214.69	259.71	1.892	197.85	274.26
s19	2.647	641.06	789.61	2.769	397.00	521.95
s20	2.600	272.85	285.80	2.594	582.89	707.09
s21	1.735	170.99	215.11	2.632	176.03	227.81
s22	1.760	166.27	213.57	2.052	216.19	281.45
s23	1.144	86.59	117.49	1.432	88.85	87.10
s24	1.530	152.72	172.76	1.919	153.96	186.20
s25	2.103	215.29	243.80	2.505	242.90	342.96
s27	1.494	131.28	154.60	1.708	141.22	176.10
s28	3.049	544.03	700.78	3.592	482.60	594.19
s29	1.990	262.57	297.37	2.154	144.60	155.02
s30	2.493	290.91	347.48	2.605	366.25	452.18
s31	1.954	246.90	312.63	2.263	351.77	435.90
s32	2.263	518.98	631.09	3.068	508.48	638.47
s33	1.145	114.15	131.25	1.461	145.59	186.73
s34	1.748	113.72	154.05	1.665	127.34	182.44
v9	2.266	403.48	513.85	2.009	411.57	517.76
v10	2.666	353.50	450.02	2.331	247.85	308.39
v11	1.324	44.33	58.21	2.126	65.25	119.82
v12	1.407	124.28	169.81	1.641	165.59	211.11
v13	1.930	207.26	256.48	2.235	197.85	246.37
v14	1.926	244.62	299.03	2.181	254.33	301.62
v16	2.073	104.40	112.97	1.936	297.66	379.62
v17	1.876	386.11	497.37	1.896	473.57	632.00
v18	2.361	238.50	283.31	2.583	123.42	129.16
v19	1.636	189.75	194.73	2.257	379.67	442.83
v20	1.547	179.14	190.27	2.197	226.10	240.28

Table 3. Participant Averages of the Variables for the Dominant and Non-Dominant limbs. Table 3 shows averages of 8 drop landings across each subject for peak vGRF normalized to body weight, Maximum Vertical Acceleration (MVA), and Minimum to Maximum Vertical Acceleration Difference (MMVAD). Participants where the left limb is listed as the dominant limb are denoted with an asterisk.

Averages of Variables for the Dominant and Non-Dominant Limb						
Participant	vGRF (ND)	MVA (ND)	MMVAD (ND)	vGRF (D)	MVA (D)	MMVAD (D)
s18	2.069	214.69	259.71	1.892	197.85	274.26
s19*	2.769	397.00	521.95	2.647	641.06	789.61
s20	2.600	272.85	285.80	2.594	582.89	707.09
s21	1.735	170.99	215.11	2.632	176.03	227.81
s22*	2.052	216.19	281.45	1.760	166.27	213.57
s23	1.144	86.59	117.49	1.432	88.85	87.10
s24	1.530	152.72	172.76	1.919	153.96	186.20
s25	2.103	215.29	243.80	2.505	242.90	342.96
s27	1.494	131.28	154.60	1.708	141.22	176.10
s28	3.049	544.03	700.78	3.592	482.60	594.19
s29*	2.154	144.60	155.02	1.990	262.57	297.37
s30	2.493	290.91	347.48	2.605	366.25	452.18
s31	1.954	246.90	312.63	2.263	351.77	435.90
s32*	3.069	508.48	638.47	2.263	518.98	631.09
s33	1.145	114.15	131.25	1.461	145.59	186.73
s34*	1.665	127.34	182.44	1.748	113.72	154.05
v9*	2.009	411.57	517.76	2.266	403.48	513.85
v10*	2.331	247.85	308.39	2.666	353.50	450.02
v11	1.324	44.33	58.21	2.126	65.25	119.82
v12*	1.641	165.59	211.11	1.407	124.28	169.81
v13	1.930	207.26	256.48	2.235	197.85	246.37
v14	1.926	244.62	299.03	2.181	254.33	301.62
v16	2.073	104.40	112.97	1.936	297.66	379.62
v17	1.876	386.11	497.37	1.896	473.57	632.00
v18	2.361	238.50	283.31	2.583	123.42	129.16
v19	1.636	189.75	194.73	2.257	379.67	442.83
v20	1.547	179.14	190.27	2.197	226.10	240.28

Table 4. Correlative Measures For MVA within the Left and Right Limb. Table 4 displays the Pearson product moment correlation coefficient for MVA to Peak vGRF, across all subjects for the left and right limbs. These r values are determined by Figures 3 and 4. Figure 3 looking at the correlation between MVA and peak vGRF for the left limb. Figure 4 looking at the correlation between MVA and peak vGRF for the right limb.

Table 4. Correlative Measures for MVA	
	Peak vGRF
MVA (Left)	r= 0.780
MVA (Right)	r= 0.590

Figure 3. Peak vGRF and MVA Correlation for the Left Limb. Figure 3 describes the correlation between the criterion variable, peak vGRF, and the first predictive variable, MVA, across all subjects for the left limb. The x-axis of the graph shows the average peak vGRF normalized to the participant's body weight for each subject across the 8 drop-landing trials. The y-axis shows the average MVA for each subject across the 8 drop-landing trials. The respective correlation value (r) and p value are listed on the right hand side of the graph.

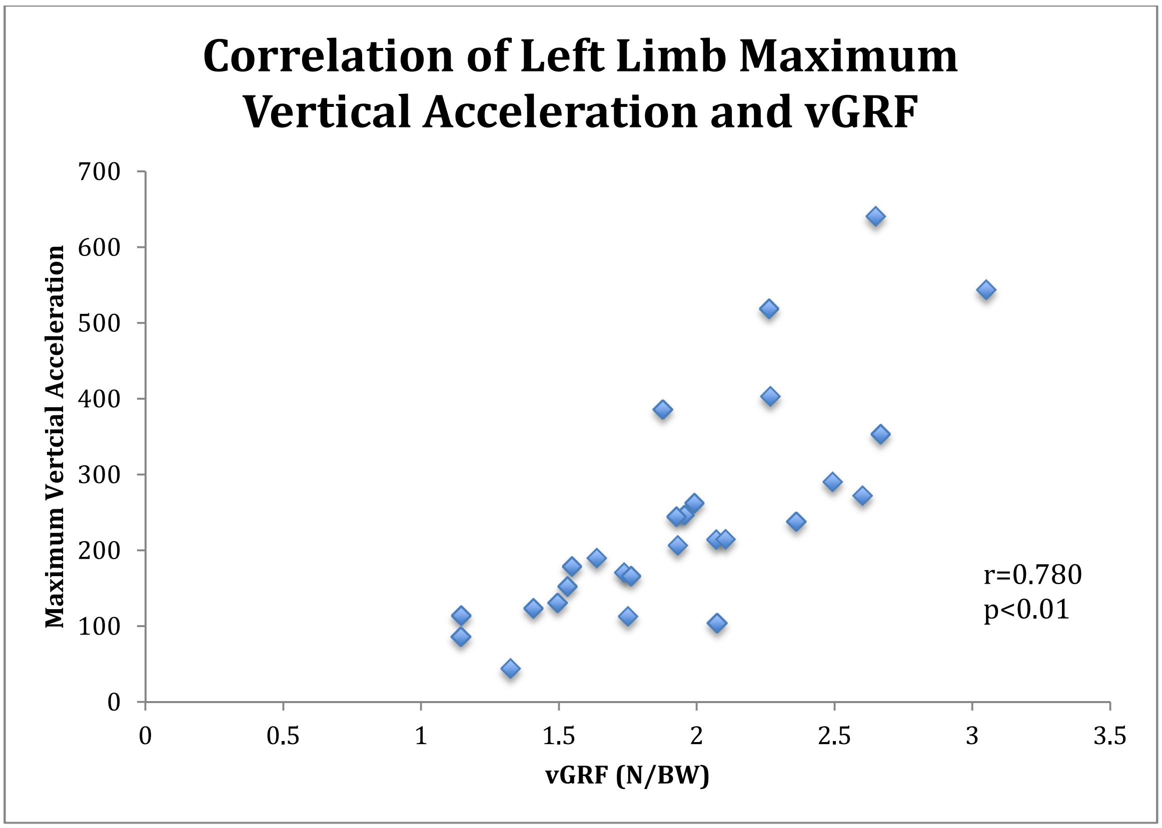

Figure 4. Peak vGRF and MVA Correlation for the Right Limb. Figure 4 describes the correlation between the criterion variable, peak vGRF, and the first predictive variable, MVA, across all subjects for the right limb. The x-axis of the graph shows the average peak vGRF normalized to the participant's body weight for each subject across the 8 drop-landing trials. The y-axis shows the average MVA for each subject across the 8 drop-landing trials. The respective correlation value (r) and p value are listed on the right hand side of the graph.

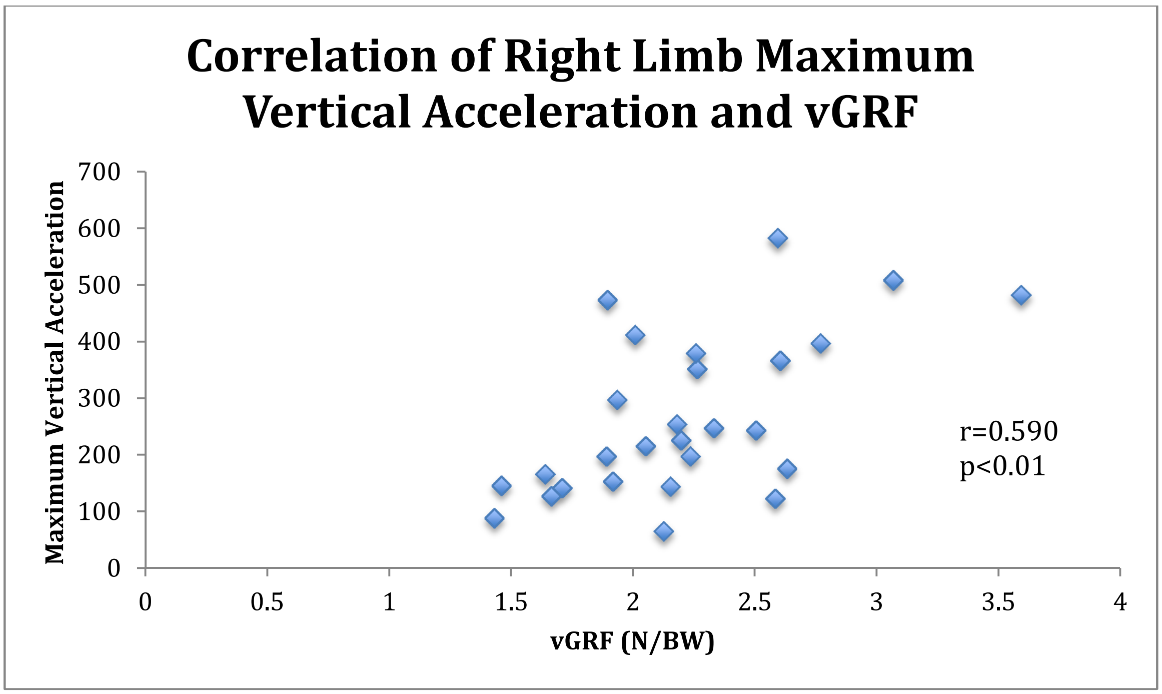

Table 5. Correlative Measures For MVA in the Non-Dominant and Dominant Limb.

Table 5 displays the Pearson product moment correlation coefficient for MVA to Peak vGRF, across all subjects in the non-dominant and dominant limb. These r values are determined by Figures 5 and 6. Figure 5 looking at the correlation between MVA and peak vGRF in the non-dominant limb. Figure 6 looking at the correlation between MVA and peak vGRF in the dominant limb.

Table 5. Correlative Measures for MVA	
	Peak vGRF
MVA (ND)	r= 0.803
MVA (DOM)	r= 0.573

Figure 5. Peak vGRF and MVA Correlation for the Non-Dominant Limb. Figure 5 describes the correlation between the criterion variable, peak vGRF, and the first predictive variable, MVA, across all subjects for the non-dominant limb. The x-axis of the graph shows the average peak vGRF normalized to the participant's body weight for each subject across the 8 drop-landing trials. The y-axis shows the average MVA for each subject across the 8 drop-landing trials. The respective correlation value (r) and p value are listed on the right hand side of the graph.

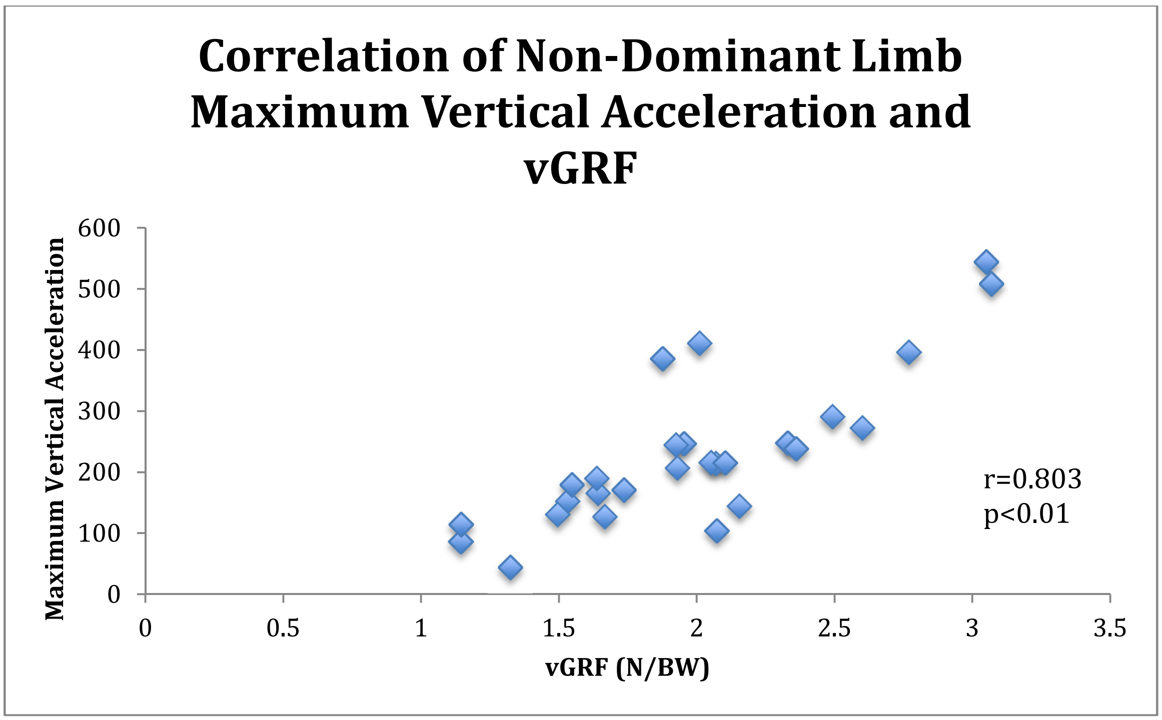

Figure 6. Peak vGRF and MVA Correlation for the Dominant Limb. Figure 6 describes the correlation between the criterion variable, peak vGRF, and the first predictive variable, MVA, across all subjects for the dominant limb. The x-axis of the graph shows the average peak vGRF normalized to the participant's body weight for each subject across the 8 drop-landing trials. The y-axis shows the average MVA for each subject across the 8 drop-landing trials. The respective correlation value (r) and p value are listed on the right hand side of the graph.

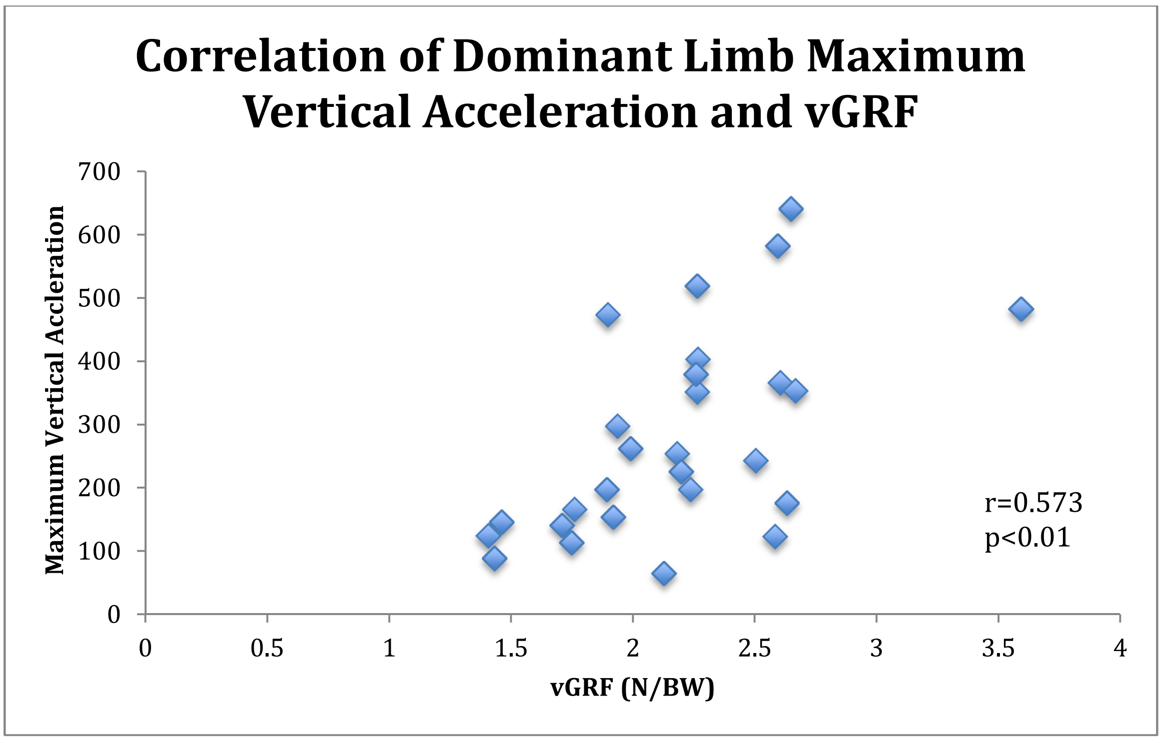

Table 6. Correlative Measures For MMVAD in the Left and Right Limb. Table 6 displays the Pearson product moment correlation coefficient for MMVAD to Peak vGRF, across all subjects in the left and right limb. These r-values are determined by Figures 7 and 8. Figure 7 looking at the correlation between MMVAD and peak vGRF in the left limb. Figure 8 looking at the correlation between MMVAD and peak vGRF in the right limb.

Table 6. Correlative Measures for MMVAD	
	Peak vGRF
MMVAD (Left)	r= 0.764
MMVAD (Right)	r= 0.576

Figure 7. Peak vGRF and MMVAD Correlation for the Left Limb. Figure 7 describes the correlation between the criterion variable, peak vGRF, and the second predictive variable, MMVAD, across all subjects. The x-axis of the graph shows the average peak vGRF normalized to the participant's body weight for each subject across the 8 drop landing trials. The y-axis shows the average MMVAD for each subject across the first 8 drop-landing trials. The respective correlation value (r) and p value are listed on the right hand side of the graph.

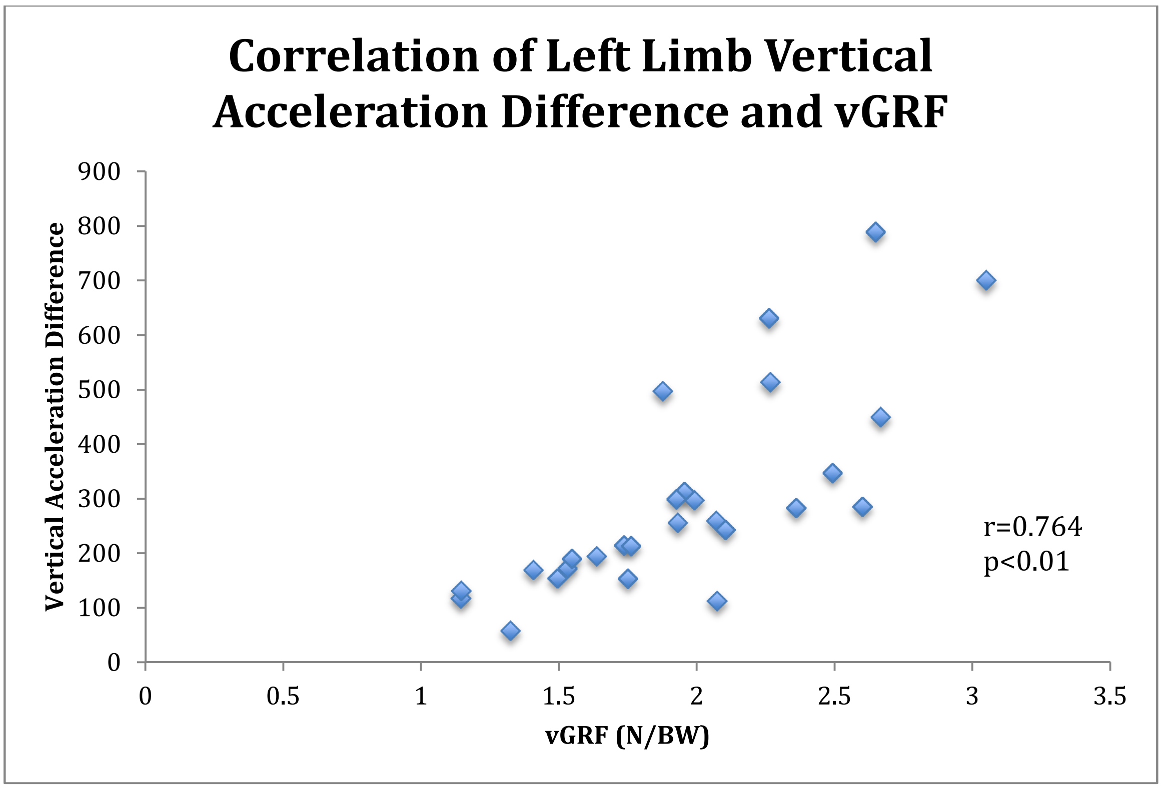

Figure 8. Peak vGRF and MMVAD Correlation for the Right Limb. Figure 8 describes the correlation between the criterion variable, peak vGRF, and the second predictive variable, MMVAD, across all subjects. The x-axis of the graph shows the average peak vGRF normalized to the participant's body weight for each subject across the 8 drop-landing trials. The y-axis shows the average MMVAD for each subject across the first 8 drop-landing trials. The respective correlation value (r) and p value are listed on the right hand side of the graph.

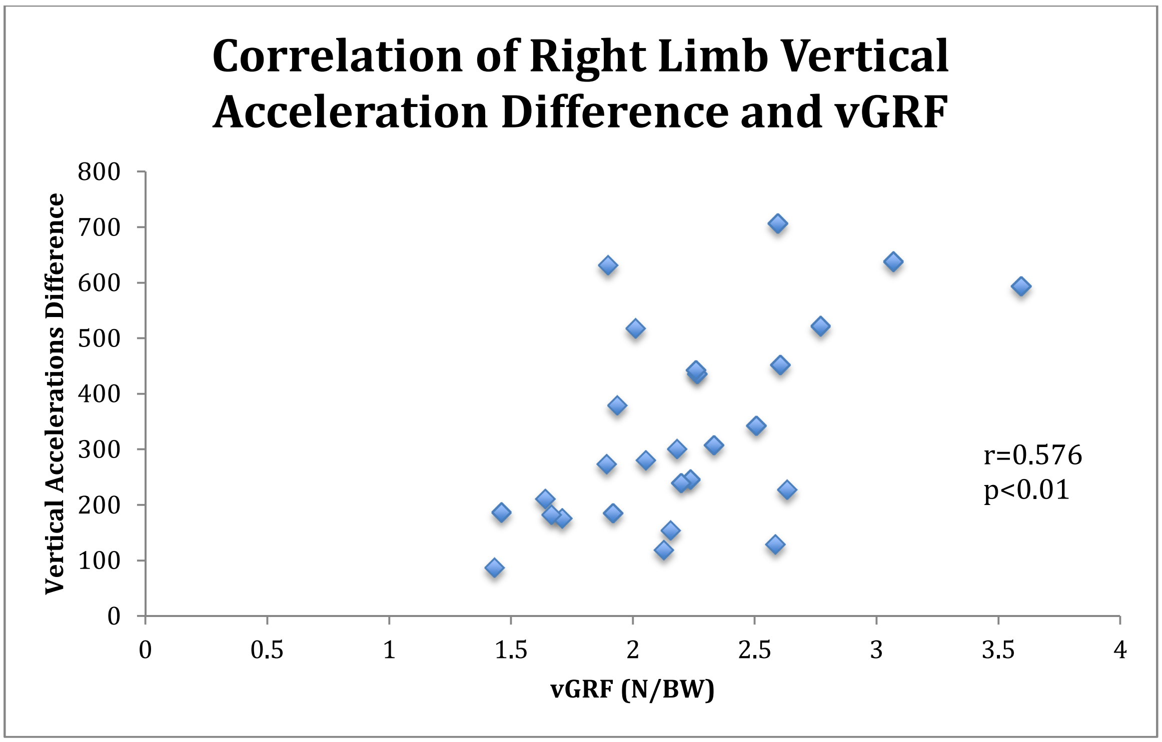

Table 7. Correlative Measures For MMVAD in the Non-Dominant and Dominant Limb. Table 7 displays the Pearson product moment correlation coefficient for MMVAD to Peak vGRF, across all subjects in the non-dominant and dominant limb. These r values are determined by Figures 9 and 10. Figure 9 looking at the correlation between MMVAD and peak vGRF in the non-dominant limb. Figure 10 looking at the correlation between MMVAD and peak vGRF in the dominant limb.

Table 7. Correlative Measures for MMVAD	
	Peak vGRF
MMVAD (ND)	r= 0.779
MMVAD (DOM)	r= 0.563

Figure 9. Peak vGRF and MMVAD Correlation for the Non-Dominant Limb. Figure 9 describes the correlation between the criterion variable, peak vGRF, and the second predictive variable, MMVAD, across all subjects. The x-axis of the graph shows the average peak vGRF normalized to the participant's body weight for each subject across the 8 drop landing trials. The y-axis shows the average MMVAD for each subject across the first 8 drop-landing trials. The respective correlation value (r) and p value are listed on the right hand side of the graph.

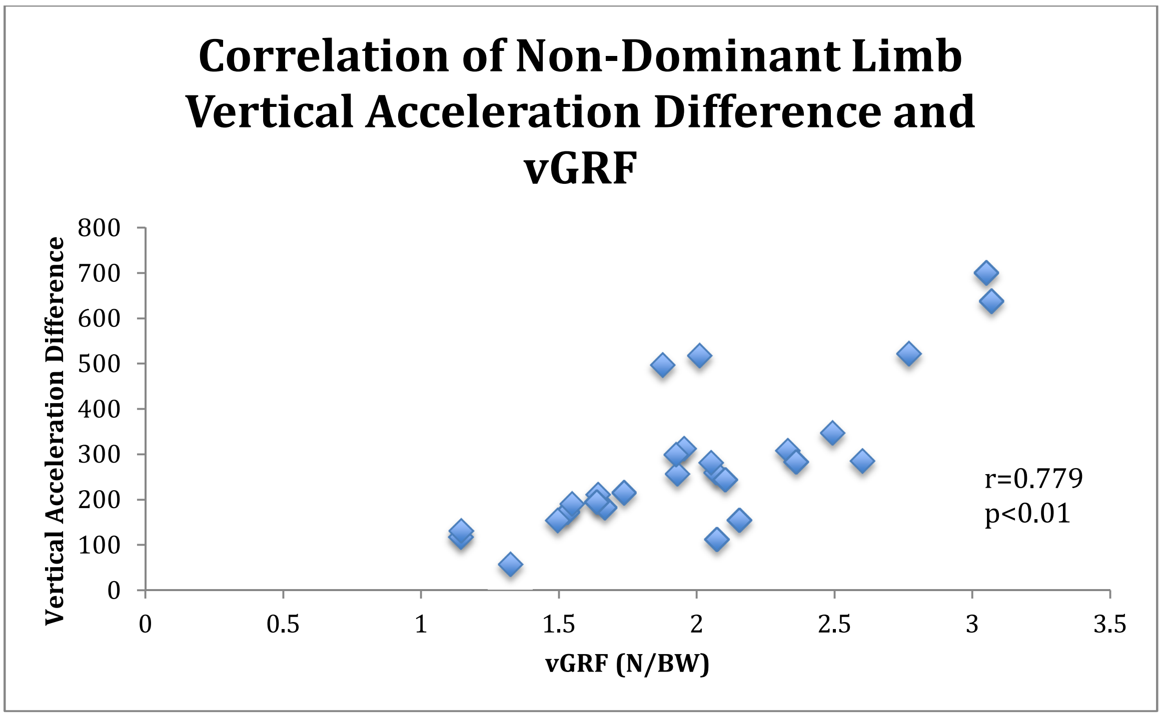

Figure 10. Peak vGRF and MMVAD Correlation for the Dominant Limb. Figure 10 describes the correlation between the criterion variable, peak vGRF, and the second predictive variable, MMVAD, across all subjects. The x-axis of the graph shows the average peak vGRF normalized to the participant's body weight for each subject across the 8 drop landing trials. The y-axis shows the average MMVAD for each subject across the first 8 drop-landing trials. The respective correlation value (r) and p value are listed on the right hand side of the graph.

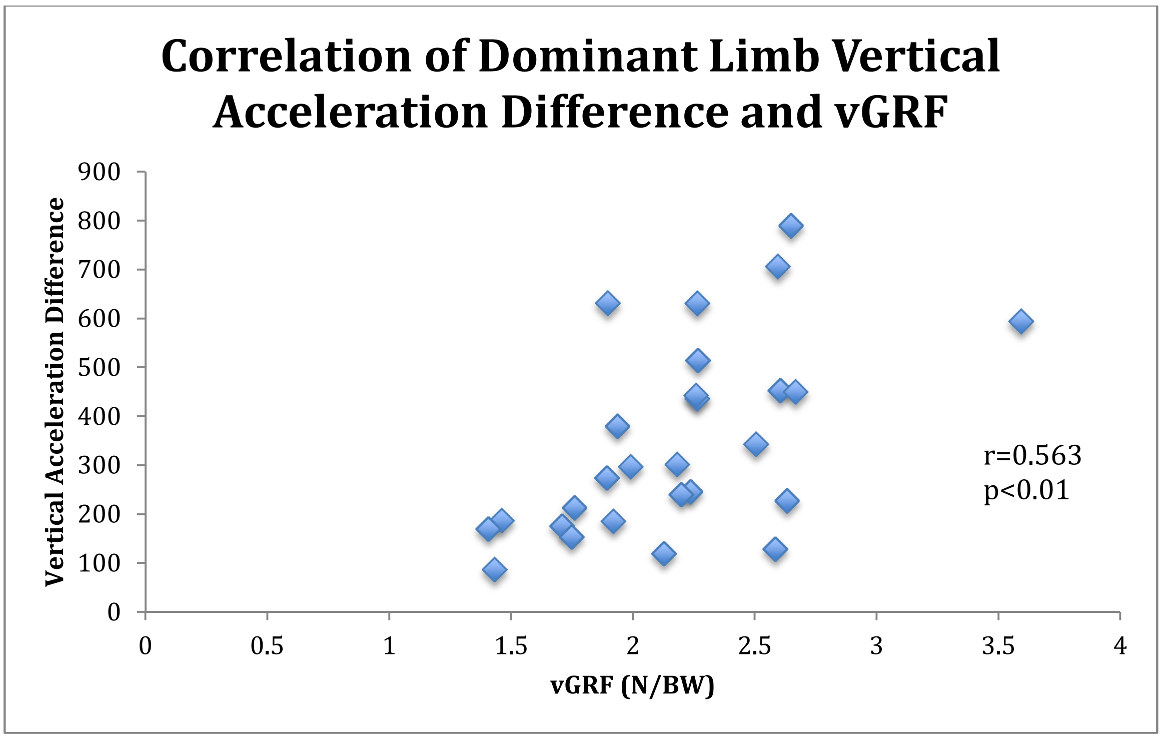

BIBLIOGRAPHY

1. Ward SH, Blackburn JT, Padua DA, et al. Quadriceps Neuromuscular Function and Jump-Landing Sagittal-Plane Knee Biomechanics After Anterior Cruciate Ligament Reconstruction. *J Athl Train*. 2018;53(2):135-143. doi:10.4085/1062-6050-306-16

2. Paterno M V., Ford KR, Myer GD, Heyl R, Hewett TE. Limb Asymmetries in Landing and Jumping 2 Years Following Anterior Cruciate Ligament Reconstruction. *Clincal J Sport Med*. 2007;17(4):258-262. doi:10.1097/JSM.0b013e31804c77ea

3. Schmitt LC, Paterno M V., Ford KR, Myer GD, Hewett TE. Strength asymmetry and landing mechanics at return to sport after anterior cruciate ligament reconstruction. *Med Sci Sports Exerc*. 2015;47(7):1426-1434. doi:10.1249/MSS.0000000000000560

4. Pfeiffer SJ, Blackburn JT, Luc-Harkey B, et al. Peak knee biomechanics and limb symmetry following unilateral anterior cruciate ligament reconstruction: Associations of walking gait and jump-landing outcomes. *Clin Biomech*. 2018. doi:10.1016/j.clinbiomech.2018.01.020

5. Trigsted SM, Cook DB, Pickett KA, Cadmus-Bertram L, Dunn WR, Bell DR. Greater fear of reinjury is related to stiffened jump-landing biomechanics and muscle activation in women after ACL reconstruction. *Knee Surgery, Sport Traumatol Arthrosc*. 2018;26(12):3682-3689. doi:10.1007/s00167-018-4950-2

6. Tsai L-C, Powers CM. Increased Hip and Knee Flexion During Landing Decreases Tibiofemoral Compressive Forces in Women Who Have Undergone Anterior Cruciate Ligament Reconstruction. doi:10.1177/0363546512471184

7. Heebner NR, Rafferty DM, Wohleber MF, et al. Landing Kinematics and Kinetics at the Knee During Different Landing Tasks. *J Athl Train*. 2017;52(12):1101-1108. doi:10.4085/1062-6050-52.11.25

8. Hébert-Losier K, Schelin L, Tengman E, Strong A, Häger CK. Curve analyses reveal altered knee, hip, and trunk kinematics during drop–jumps long after anterior cruciate ligament rupture. *Knee*. 2018;25(2):226-239. doi:10.1016/j.knee.2017.12.005

9. Padua DA, Marshall SW, Boling MC, Thigpen CA, Garrett Jr WE, Beutler AI. The Landing Error Scoring System (LESS) Is a Valid and Reliable Clinical Assessment Tool of Jump-Landing Biomechanics The JUMP-ACL Study Department of Exercise and Sport Science and the. *Am J Sports Med*. 2009;37(10). doi:10.1177/0363546509343200

10. Munro A, Herrington L. The effect of videotape augmented feedback on drop jump landing strategy: Implications for anterior cruciate ligament and patellofemoral joint injury prevention. *Knee*. 2014;21(5):891-895. doi:10.1016/j.knee.2014.05.011

11. Nyman E�, Armstrong CW. Real-time feedback during drop landing training improves subsequent frontal and sagittal plane knee kinematics. 2015. doi:10.1016/j.clinbiomech.2015.06.018

12. Myer GD, Stroube BW, DiCesare CA, et al. Augmented Feedback Supports Skill Transfer and Reduces High-Risk Injury Landing Mechanics A Double-Blind, Randomized Controlled Laboratory Study. doi:10.1177/0363546512472977

13. Ziebart C, Giangregorio LM, Gibbs JC, Levine IC, Tung J, Laing AC. Measurement of peak impact loads differ between accelerometers-Effects of system operating range and sampling rate. doi:10.1016/j.jbiomech.2017.04.022

14. Luc-Harkey BA, Franz JR, Blackburn JT, Padua DA, Hackney AC, Pietrosimone B. Real-time biofeedback can increase and decrease vertical ground reaction force, knee flexion excursion, and knee extension moment during walking in individuals with anterior cruciate ligament reconstruction. *J Biomech*. 2018. doi:10.1016/j.jbiomech.2018.05.043

15. Fortune E, Morrow MMB, Kaufman KR. Assessment of gait kinetics using triaxial accelerometers. *J Appl Biomech*. 2014;30(5):668-674. doi:10.1123/JAB.2014-0037

16. Ngoh KJH, Gouwanda D, Gopalai AA, Chong YZ. Estimation of vertical ground reaction force during running using neural network model and uniaxial accelerometer. *J Biomech*. 2018;76:269-273. doi:10.1016/j.jbiomech.2018.06.006

17. Rowlands A V., Stiles VH. Accelerometer counts and raw acceleration output in relation to mechanical loading. *J Biomech*. 2012;45(3):448-454. doi:10.1016/j.jbiomech.2011.12.006

18. Sheerin KR, Reid D, Besier TF. The measurement of tibial acceleration in runners—A review of the factors that can affect tibial acceleration during running and evidence-based guidelines for its use. *Gait Posture*. 2019;67(May 2018):12-24. doi:10.1016/j.gaitpost.2018.09.017

19. Butler RJ, Minick KI, Ferber R, Underwood F. Gait mechanics after ACL reconstruction: Implications for the early onset of knee osteoarthritis. *Br J Sports Med*. 2009. doi:10.1136/bjsm.2008.052522

20. Slater L V, Hart JM, Kelly AR, Kuenze CM. Progressive Changes in Walking Kinematics and Kinetics After Anterior Cruciate Ligament Injury and Reconstruction: A Review and Meta-Analysis. *J Athl Train*. 2017;52(9):847-860.

doi:10.4085/1062-6050-52.6.06

21. Clarke SB, Kenny IC, Harrison AJ. Dynamic knee joint mechanics after anterior cruciate ligament reconstruction. *Med Sci Sports Exerc*. 2015;47(1):120-127. doi:10.1249/MSS.0000000000000389

22. Sharifi M, Shirazi-Adl A, Marouane H. Computation of the role of kinetics, kinematics, posterior tibial slope and muscle cocontraction on the stability of ACL-deficient knee joint at heel strike – Towards identification of copers from non-copers. *J Biomech*. 2018;77:171-182. doi:10.1016/j.jbiomech.2018.07.003

23. Hadizadeh M, Amri S, Mohafez H, Roohi SA, Mokhtar AH. Gait analysis of national athletes after anterior cruciate ligament reconstruction following three stages of rehabilitation program: Symmetrical perspective. *Gait Posture*. 2016. doi:10.1016/j.gaitpost.2016.05.002

24. Kaur M, Ribeiro DC, Theis JC, Webster KE, Sole G. Movement Patterns of the Knee During Gait Following ACL Reconstruction: A Systematic Review and Meta-Analysis. *Sport Med*. 2016. doi:10.1007/s40279-016-0510-4

25. Pietrosimone B, Nissman D, Padua DA, et al. Associations between cartilage proteoglycan density and patient outcomes 12 months following anterior cruciate ligament reconstruction. *Knee*. 2018;25(1):118-129. doi:10.1016/j.knee.2017.10.005

26. Pfeiffer SJ, Spang J, Nissman D, et al. *Gait Mechanics and T1ρ MRI of Tibiofemoral Cartilage 6 Months Post ACL Reconstruction*.; 2018. doi:10.1249/MSS.0000000000001834

27. Goerger BM, Marshall SW, Beutler AI, Blackburn JT, Wilckens JH, Padua DA. Anterior cruciate ligament injury alters preinjury lower extremity biomechanics in the injured and uninjured leg: The JUMP-ACL study. *Br J Sports Med*. 2015;49(3):188-195. doi:10.1136/bjsports-2013-092982

28. Pamukoff DN, Montgomery MM, Holmes SC, Moffit TJ, Garcia SA, Vakula MN. Association between gait mechanics and ultrasonographic measures of femoral cartilage thickness in individuals with ACL reconstruction. *Gait Posture*. 2018;65(April):221-227. doi:10.1016/j.gaitpost.2018.07.174

29. Hewett TE, Myer GD, Ford KR, et al. Biomechanical measures of neuromuscular control and valgus loading of the knee predict anterior cruciate ligament injury risk in female athletes: A prospective study. *Am J Sports Med*. 2005;33(4):492-501. doi:10.1177/0363546504269591

30. Kim SY, Spritzer CE, Utturkar GM, Toth AP, Garrett WE, DeFrate LE. Knee Kinematics During Noncontact Anterior Cruciate Ligament Injury as Determined

From Bone Bruise Location. *Am J Sports Med*. 2015;43(10):2515-2521. doi:10.1177/0363546515594446

31. Kaeding CC, Léger-St-Jean B, Magnussen RA. Epidemiology and Diagnosis of Anterior Cruciate Ligament Injuries. *Clin Sports Med*. 2017;36(1):1-8. doi:10.1016/j.csm.2016.08.001

32. Gornitzky AL, Lott A, Yellin JL, Fabricant PD, Lawrence JT, Ganley TJ. Sport-Specific Yearly Risk and Incidence of Anterior Cruciate Ligament Tears in High School Athletes: A Systematic Review and Meta-analysis. *Am J Sports Med*. 2016;44(10):2716-2723. doi:10.1177/0363546515617742

33. Von Porat A, Roos EM, Roos H. High prevalence of osteoarthritis 14 years after an anterior cruciate ligament tear in male soccer players: A study of radiographic and patient relevant outcomes. *Ann Rheum Dis*. 2004;63(3):269-273. doi:10.1136/ard.2003.008136

34. Rosquist PG, Collins G, Merrell AJ, et al. Estimation of 3D Ground Reaction Force Using Nanocomposite Piezo-Responsive Foam Sensors During Walking. *Ann Biomed Eng*. 2017. doi:10.1007/s10439-017-1852-2

35. Blackburn JT, Pietrosimone B, Harkey MS, Luc BA, Pamukoff DN. Inter-limb differences in impulsive loading following anterior cruciate ligament reconstruction in females. *J Biomech*. 2016. doi:10.1016/j.jbiomech.2016.07.030

36. Pietrosimone B, Blackburn JT, Harkey MS, et al. Greater Mechanical Loading during Walking Is Associated with Less Collagen Turnover in Individuals with Anterior Cruciate Ligament Reconstruction. *Am J Sports Med*. 2016;44(2):425-432. doi:10.1177/0363546515618380

37. Wellsandt E, Gardinier ES, Manal K, Axe MJ, Buchanan TS, Snyder-Mackler L. Decreased Knee Joint Loading Associated with Early Knee Osteoarthritis after Anterior Cruciate Ligament Injury. *Am J Sports Med*. 2016;44(1):143-151. doi:10.1177/0363546515608475

38. Lohmander LS, Östenberg A, Englund M, Roos H. High prevalence of knee osteoarthritis, pain, and functional limitations in female soccer players twelve years after anterior cruciate ligament injury. *Arthritis Rheum*. 2004;50(10):3145-3152. doi:10.1002/art.20589

39. Su F, Pedoia V, Teng HL, et al. The association between MR T1ρ and T2 of cartilage and patient-reported outcomes after ACL injury and reconstruction. *Osteoarthr Cartil*. 2016;24(7):1180-1189. doi:10.1016/j.joca.2016.01.985

40. Lewek M, Rudolph K, Axe M, Snyder-Mackler L. The effect of insufficient quadriceps strength on gait after anterior cruciate ligament reconstruction. *Clin*

Biomech. 2002;17(1):56-63. doi:10.1016/S0268-0033(01)00097-3

41. Teng HL, Wu D, Su F, et al. Gait Characteristics Associated With a Greater Increase in Medial Knee Cartilage T1ρand T2Relaxation Times in Patients Undergoing Anterior Cruciate Ligament Reconstruction. *Am J Sports Med*. 2017;45(14):3262-3271. doi:10.1177/0363546517723007

42. Stöggl T, Martiner A. Validation of Moticon's OpenGo sensor insoles during gait, jumps, balance and cross-country skiing specific imitation movements. *J Sports Sci*. 2017;35(2):196-206. doi:10.1080/02640414.2016.1161205

43. Khurelbaatar T, Kim K, Lee SK, Kim YH. Consistent accuracy in whole-body joint kinetics during gait using wearable inertial motion sensors and in-shoe pressure sensors. *Gait Posture*. 2015;42(1):65-69. doi:10.1016/j.gaitpost.2015.04.007

44. Zhang JH, An WW, Au IPH, Chen TL, Cheung RTH. Comparison of the correlations between impact loading rates and peak accelerations measured at two different body sites: Intra- and inter-subject analysis. *Gait Posture*. 2016;46:53-56. doi:10.1016/j.gaitpost.2016.02.002

45. Faber GS, Kingma I, Martin Schepers H, Veltink PH, van Dieën JH. Determination of joint moments with instrumented force shoes in a variety of tasks. *J Biomech*. 2010;43(14):2848-2854. doi:10.1016/j.jbiomech.2010.06.005

46. Khurelbaatar T, Kim K, Lee SK, Kim YH. Consistent accuracy in whole-body joint kinetics during gait using wearable inertial motion sensors and in-shoe pressure sensors. *Gait Posture*. 2015;42(1):65-69. doi:10.1016/j.gaitpost.2015.04.007

47. Sabatini AM. Estimating three-dimensional orientation of human body parts by inertial/magnetic sensing. *Sensors*. 2011;11(2):1489-1525. doi:10.3390/s110201489

48. Han SH, Kim CO, Kim KJ, et al. Quantitative analysis of the bilateral coordination and gait asymmetry using inertial measurement unit-based gait analysis. *PLoS One*. 2019;14(10):1-11. doi:10.1371/journal.pone.0222913

49. SparkFun Electronics. https://www.sparkfun.com/. Accessed November 27, 2019.

50. MTi 600-series. https://www.xsens.com/products/mti-600-series. Accessed November 27, 2019.

51. Renner KE, Blaise Williams DS, Queen RM. The reliability and validity of the Loadsol® under various walking and running conditions. *Sensors (Switzerland)*. 2019;19(2):1-14. doi:10.3390/s19020265

52. Patrick K, Donovan L. Test–retest reliability of the Tekscan® F-Scan® 7 in-shoe plantar pressure system during treadmill walking in healthy recreationally active individuals. *Sport Biomech*. 2018;17(1):83-97. doi:10.1080/14763141.2017.1355010

53. Jarchi D, Pope J, Lee TKM, Tamjidi L, Mirzaei A, Sanei S. A Review on Accelerometry-Based Gait Analysis and Emerging Clinical Applications. *IEEE Rev Biomed Eng*. 2018;11(c):177-194. doi:10.1109/RBME.2018.2807182

54. Accelerometers | Mouser. https://www.mouser.com/Search/Refine?N=18357019. Accessed January 27, 2020.

55. Neugebauer JM, Hawkins DA, Beckett L. Estimating Youth Locomotion Ground Reaction Forces Using an Accelerometer-Based Activity Monitor. *PLoS One*. 2012;7(10). doi:10.1371/journal.pone.0048182

56. Moe-Nilssen R, Helbostad JL. Estimation of gait cycle characteristics by trunk accelerometry. *J Biomech*. 2004;37(1):121-126. doi:10.1016/S0021-9290(03)00233-1

57. Faul F, Erdfelder E, Lang A-G, Buchner A. G*Power 3: A flexible statistical power analysis program for the social, behavioral, and biomedical sciences. *Behav Res Methods*. 2007;39(2):175-191. doi:10.3758/BF03193146

58. Mukaka M. A guide to appropriate use of Correlation coefficient in medical research. *Malawi Med J*. 2012;24(3):69-71.